*"We stand on the shoulders of giants,*
*drawing wisdom from the works of*
*those who came before us."*

*– Sir Isaac Newton*

# 2

# Formalism and Statistical Methodology

Neutrino non-standard interactions (NSIs) represent a fascinating and relatively unexplored frontier in the realm of particle physics. Unlike the well-known weak interactions that neutrinos undergo through the exchange of W and Z bosons, NSIs involve interactions beyond the scope of the Standard Model of particle physics. These interactions could be mediated by hypothetical particles or new physics scenarios, potentially opening doors to a deeper understanding of neutrino properties and their role in the universe. Neutrino NSIs could manifest in various ways, altering the expected neutrino oscillation patterns, affecting neutrino propagation through matter, and even modifying their interactions with other particles. Detecting and characterizing these NSIs present both theoretical and experimental challenges, but their study holds the promise of unveiling new insights into the fundamental nature of neutrinos and potentially shedding light on the mysteries beyond Standard-Model physics.

## 2.1 Non Standard interactions of neutrinos

The joint discovery of neutrino oscillations by the Super–Kamiokande (SK)[1] and Sudbury Neutrino Observatory (SNO)[2] has opened up a new avenue for probing physics beyond the Standard Model (BSM). Neutrino oscillations unequivocally confirm the neutrino's mass and offer the initial experimental insight into BSM physics. Various neutrino experiments extensively investigate the parameters related to neutrino oscillations [3–6]. Neutrinos serve as promising portals to explore BSM physics in the leptonic sector. BSM models, which elucidate neutrino masses and mixing, frequently explore novel, undiscovered couplings of neutrinos referred to as non–standard interactions (NSIs). Given the unparalleled accuracy and precision achieved by current and forthcoming neutrino experiments, these lesser-known effects on neutrino oscillations could significantly shape the potential outcomes of these experiments. In this study, we primarily investigate the ramifications of scalar-mediated NSIs on the measurements of the leptonic phase $\delta_{CP}$ within three long-baseline (LBL) neutrino experiments: DUNE [81], T2HK [82], and T2HKK [83]. Employing a model-independent approach, we conduct a synergistic analysis that combines these LBL experiments to scrutinize the influence of scalar NSIs.

In the precision-driven era of neutrino physics, ongoing and forthcoming neutrino experiments are dedicated to achieving the utmost accuracy in measuring neutrino mixing parameters. These experiments have a central objective: to address the three key unknowns within the neutrino sector. These unknowns encompass the hierarchy of neutrino masses [84], the octant of the mixing angle $\theta_{23}$ [85], and the determination of the CP phase ($\delta_{CP}$) within the leptonic sector [86]. The robust nature of these ongoing and future neutrino experiments endows them with sensitivity to the subtler effects of neutrinos. One such effect is Non-Standard Interactions (NSI), which can exert a significant influence on the measurement of oscillation parameters in diverse neutrino experiments. Originally introduced with the concept of neutrino interactions through a vector mediator with environmental fermions [12], vector-mediated NSIs manifest as matter potential terms within the neutrino oscillation Hamiltonian. Extensively explored [55–58, 87], vector-mediated NSIs offer a compelling avenue to explore physics beyond the Standard Model, potentially reshaping the physics reach of various neutrino experiments [88–112], with active exploration of these effects [113–129]. A comprehensive overview of constraints on vector NSI parameters globally can be found in [130, 131].

### 2.1.1 Vector Non Standard Interaction

In the realm of Beyond the Standard Model (BSM) physics, in addition to the well-known charged-current (CC) and neutral-current (NC) weak interactions, there exists the possibility of vector-mediated Non-Standard Interactions (NSI) of both CC and NC varieties. CC-type vector NSIs have an impact on neutrino production and detection, while NC-type vector NSIs influence the propagation of neutrinos. The effective Lagrangian for both CC and NC types is expressed in the following forms,

$$\mathcal{L}_{NC}^{VNSI} = -2\sqrt{2}G_F \sum_{f,P,\alpha,\beta} \epsilon_{\alpha\beta}^{f,P}(\bar{\nu}_\alpha \gamma^\mu P_L \nu_\beta)(\bar{f}\gamma_\mu P f) \tag{2.1}$$

$$\mathcal{L}_{CC}^{VNSI} = -2\sqrt{2}G_F \sum_{f,P,\alpha,\beta} \epsilon_{\alpha\beta}^{f,P}(\bar{\nu}_\alpha \gamma^\mu P_L l_\beta)(\bar{f}\gamma_\mu P f'). \tag{2.2}$$

The $\epsilon$ terms measure the magnitude of non-standard interactions (NSI) relative to the weak scale. The fermions of matter, denoted as $f, f' \in (e, u, d)$, and the left and right chiral operators, represented by $P \in (P_L, P_R)$, play crucial roles. Introducing a NSI term, as illustrated in equations 2.2 and 2.1, allows the effective neutrino Hamiltonian to be formulated as follows,

$$\mathcal{H}_{VNSI} = \mathcal{H}_{matter} + V_{VNSI}. \tag{2.3}$$

Where, $\mathcal{H}_{matter}$ is the standard neutrino matter Hamiltonian and $V_{VNSI}$ is generally represented as,

$$V_{VNSI} = A \begin{pmatrix} \epsilon_{ee} & \epsilon_{e\mu} & \epsilon_{e\tau} \\ \epsilon_{\mu e} & \epsilon_{\mu\mu} & \epsilon_{\mu\tau} \\ \epsilon_{\tau e} & \epsilon_{\tau\mu} & \epsilon_{\tau\tau} \end{pmatrix}, \tag{2.4}$$

with $A = 2\sqrt{2}G_F N_e E$ and $N_e$ being electron number density.

### 2.1.2 Scalar Non Standard Interaction: the concept & formalism

Experiments [3–6] spanning a wide array of baselines and energies have validated the concept of neutrino oscillations. This phenomenon establishes that neutrinos, owing to their nonzero masses [46], can undergo flavor transformations. The empirical data gathered from these experiments unequivocally demonstrate that the neutrino flavors

$(\nu_e, \nu_\mu, \nu_\tau)$ are actually composed of superpositions of their mass states $(\nu_1, \nu_2, \nu_3)$ possessing masses $m_1, m_2, m_3$ correspondingly. The interplay between these flavor and mass eigenstates is dictated by a $3 \times 3$ matrix known as the Pontecorvo-Maki-Nakagawa-Sakata (PMNS) matrix, denoted as $\mathcal{U}$ [45, 46, 132, 133].

$$\mathcal{U} = \begin{pmatrix} 1 & 0 & 0 \\ 0 & c_{23} & s_{23} \\ 0 & -s_{23} & c_{23} \end{pmatrix} \begin{pmatrix} c_{13} & 0 & s_{13}e^{-i\delta_{CP}} \\ 0 & 1 & 0 \\ -s_{13}e^{i\delta_{CP}} & 0 & c_{13} \end{pmatrix} \begin{pmatrix} c_{12} & s_{12} & 0 \\ -s_{12} & c_{12} & 0 \\ 0 & 0 & 1 \end{pmatrix} . \quad (2.5)$$

Here, $s_{ij} = \sin\theta_{ij}$, $c_{ij} = \cos\theta_{ij}$, and $\delta_{CP}$ represents the Dirac-type CP phase. This form is referred to as the PDG parameterization [134] of the PMNS matrix. Furthermore, if neutrinos are regarded as Majorana particles, two additional phases known as Majorana phases can emerge. However, these phases have no impact on neutrino oscillations as they can be absorbed as a shared phase in the neutrino Hamiltonian. This specific PMNS matrix parameterization will be employed consistently throughout the course of this study.

Within the context of Standard Model interactions, neutrinos engage with matter solely through weak interactions, facilitated by a mediator such as a $W^\pm$ or Z boson [135]. The formulation of the effective Lagrangian governing these interactions is expressed as [12, 136, 137],

$$\mathcal{L}_{\text{cc}}^{\text{eff}} = -\frac{4G_F}{\sqrt{2}} \left[\overline{\nu_e}(p_3)\gamma_\mu P_L \nu_e(p_2)\right] \left[\overline{e}(p_1)\gamma^\mu P_L e(p_4)\right] . \quad (2.6)$$

In this context, $P_L$ and $P_R$ denote the left and right chiral projection operators, respectively, defined as $P_L = (1 - \gamma_5)/2$ and $P_R = (1 + \gamma_5)/2$. The quantities $p_i$ represent the momenta of incoming and outgoing states, while $G_F$ represents the Fermi constant.

Typically, the effects of neutrinos interacting with matter stem from the forward scattering of neutrinos, where there is negligible momentum transfer between the initial and final states. These effects manifest as matter potentials within the neutrino Hamiltonian, namely $V_{\text{CC}} = \pm\sqrt{2}G_F n_e$ and $V_{\text{NC}} = \pm\frac{G_F n_n}{\sqrt{2}}$. In this context, $V_{\text{CC}}$ and $V_{\text{NC}}$ represent the matter potentials originating from charged-current (CC) and neutral-current (NC) interactions of neutrinos with matter, respectively. The positive sign arises from neutrino-matter interactions, while the negative sign corresponds to antineutrino-matter interactions. Notably, the matter potential associated with NC interactions ($V_{\text{NC}}$) does not influence neutrino oscillations, as it merely introduces a common phase

within the neutrino Hamiltonian. Therefore, the effective Hamiltonian ($\mathcal{H}_{matter}$) describing neutrino oscillations within a matter environment can be expressed as [13],

$$\mathcal{H}_{matter} \approx E_\nu + \frac{MM^\dagger}{2E_\nu} \pm V_{\rm SI}\,, \tag{2.7}$$

In this context, where $E_\nu$ represents the energy of the neutrino, M denotes the mass matrix of neutrinos, and $V_{\rm SI}$ signifies the matter potential due to the effects of neutrino-matter interactions. It is worth reiterating that the polarity of the term '$V_{SI}$' arises from neutrino or antineutrino modes. The neutrino mass matrix $M$ in the flavor basis takes the form of $\mathcal{U}D_\nu\mathcal{U}^\dagger$, wherein $D_\nu$ denotes the diagonal mass matrix of neutrinos, specifically $D_\nu \equiv {\rm diag}(m_1, m_2, m_3)$. Consequently, the simplified effective Hamiltonian ($\mathcal{H}_{\rm eff}$) governing neutrino oscillations within a matter medium can be derived as,

$$\mathcal{H}_{\rm eff} = E_\nu + \frac{1}{2E_\nu}\mathcal{U}{\rm diag}(0, \Delta m^2_{21}, \Delta m^2_{31})\mathcal{U}^\dagger + {\rm diag}(V_{\rm CC}, 0, 0)\,, \tag{2.8}$$

where, $\Delta m^2_{ij} \equiv m^2_i - m^2_j$ are the neutrino mass-squared differences. The quantity $V_{\rm CC} \equiv \pm\sqrt{2}G_F n_e$ is the effective matter potential due to the coherent elastic forward scattering of neutrinos with electrons in the matter through the SM gauge boson $W$.

While the exploration of vector-mediated NSIs has been extensive, alternative non-standard effects can originate from different sources. One intriguing possibility involves the coupling of neutrinos with a scalar particle, such as the Higgs boson, which possesses nonzero vacuum expectation values contributing to neutrino mass generation. The prospect of neutrino coupling with a scalar adds an interesting dimension to the study. The effective Lagrangian governing such a scalar NSI scenario can be formulated as,

$$\mathcal{L}^{\rm S}_{\rm eff} \;=\; \frac{y_f y_{\alpha\beta}}{m^2_\phi}(\bar{\nu}_\alpha(p_3)\nu_\beta(p_2))(\bar{f}(p_1)f(p_4))\,, \tag{2.9}$$

where,

- $\alpha$, $\beta$ refer to the neutrino flavours e, $\mu$, $\tau$,
- $f$ = e, u, d indicate the matter fermions, (e: electron, u: up-quark, d: down-quark),
- $\bar{f}$ is for corresponding anti fermions,
- $y_{\alpha\beta}$ is the Yukawa couplings of the neutrinos with the scalar mediator $\phi$,
- $y_f$ is the Yukawa coupling of $\phi$ with $f$, and,

- $m_\phi$ is the mass of the scalar mediator $\phi$.

Analyzing equation 2.9, it becomes evident that the effective Lagrangian is constituted of Yukawa terms, rendering it incapable of transforming into vector currents. Consequently, the presence of scalar NSI does not translate into a contribution to the matter potential term within the neutrino Hamiltonian. Instead, it could manifest as a perturbation to the neutrino mass term contingent on the medium[7]. Throughout this paper, we will employ the subscript "SNSI" to denote quantities that encompass the influence of scalar NSI.

The corresponding Dirac equation, when accommodating these novel scalar interactions, can be simplified [7] as,

$$\bar{\nu}_\beta \left[ i\partial_\mu \gamma^\mu + \left( M_{\beta\alpha} + \frac{\sum_f n_f y_f y_{\alpha\beta}}{m_\phi^2} \right) \right] \nu_\alpha = 0 \,, \tag{2.10}$$

where, $n_f$ is the number density of the environmental fermions.

It's apparent that the influence of scalar NSI is observed in the Dirac equation through its association with the mass term. The effective Hamiltonian [11, 14, 15], which accounts for the impact of scalar NSI, will present a modified version of Eq. 2.8, as demonstrated below,

$$\mathcal{H}_{\rm SNSI} \approx E_\nu + \frac{M_{\rm eff} M_{\rm eff}^\dagger}{2E_\nu} \pm V_{\rm SI} \,. \tag{2.11}$$

In this equation, $M_{\rm eff}$ represents the comprehensive mass matrix encompassing both the conventional mass matrix $M$ and the influence arising from scalar NSI, denoted as $M_{SNSI} \equiv \sum_f n_f y_f y_{\alpha\beta}/m_\phi^2$. It can be expressed as the sum of these components:

$$M_{\rm eff} = M + M_{\rm SNSI} \tag{2.12}$$

The neutrino mass matrix (denoted as $\equiv \mathcal{U}' \mathcal{D}_\nu \mathcal{U}'^\dagger$) can be diagonalized through the action of a mixing matrix $U' \equiv PUQ^\dagger$. In this context, Q represents a Majorana rephasing matrix, which can be absorbed as $QD_\nu Q^\dagger = D_\nu$. The matrix P is an unphysical diagonal rephasing matrix that cannot be eliminated through rotation. We carry out a rotation on matrix P by incorporating the contribution arising from the scalar NSI. As a result, $M_{\rm eff}$ can be expressed as follows:

$$M_{eff} \equiv U D_\nu U^\dagger + P^\dagger M_{SNSI} P \equiv M + \delta M \tag{2.13}$$

We introduce the term $\delta M$ to encompass the perturbative contribution of scalar NSI, incorporating the unphysical rephasing matrix P as well. Our aim is to establish

an effective and comprehensive form for $\delta M$ that simplifies the study of individual matrix elements in conjunction with the neutrino mass matrix. To achieve this, we parameterize $\delta M$ as follows,

$$\delta M \equiv \sqrt{|\Delta m^2_{31}|} \begin{pmatrix} \eta_{ee} & \eta_{e\mu} & \eta_{e\tau} \\ \eta_{\mu e} & \eta_{\mu\mu} & \eta_{\mu\tau} \\ \eta_{\tau e} & \eta_{\tau\mu} & \eta_{\tau\tau} \end{pmatrix} . \tag{2.14}$$

We adopt the scaling factor $\sqrt{|\Delta m^2_{31}|}$ as a characteristic measure. The elements $\eta_{\alpha\beta}$, devoid of dimensions, serve to quantify the impacts of scalar NSI.

The requirement for the neutrino Hamiltonian to be Hermitian necessitates real diagonal elements and complex off-diagonal elements. These can be parameterized as follows:

$$\eta_{\alpha\beta} = |\eta_{\alpha\beta}| e^{i\phi_{\alpha\beta}}; \qquad \alpha \neq \beta. \tag{2.15}$$

For the scope of this study, we have employed a diagonal form for $\delta M$, thus preserving the Hermitian nature of the Hamiltonian. This approach facilitates the examination of scalar NSI elements across diverse probability channels. The elements $\eta_{\alpha\beta}$ serve as quantifiers for interaction strength, and their investigation can be extended to a range of neutrino experiments. As of now, conclusive bounds for these elements remain elusive, prompting the anticipation that constraints will emerge from the outcomes of various neutrino experiments.

We have explored three distinct scenarios, each featuring a single nonzero diagonal element at a time. The expressions for $M_{\text{eff}}$ that we utilize to compute the modified Hamiltonian for these three scenarios are provided below,

$$\text{Case I}: M_{\text{eff}} = U \text{diag}\,(m_1, m_2, m_3)\, U^\dagger + \sqrt{|\Delta m^2_{31}|}\ \text{diag}\,(\eta_{\text{ee}}, 0, 0) \tag{2.16}$$

$$\text{Case II}: M_{\text{eff}} = U \text{diag}\,(m_1, m_2, m_3)\, U^\dagger + \sqrt{|\Delta m^2_{31}|}\ \text{diag}\,(0, \eta_{\mu\mu}, 0) \tag{2.17}$$

$$\text{Case III}: M_{\text{eff}} = U \text{diag}\,(m_1, m_2, m_3)\, U^\dagger + \sqrt{|\Delta m^2_{31}|}\ \text{diag}\,(0, 0, \eta_{\tau\tau}) \tag{2.18}$$

Notably, $\mathcal{H}_{\text{SNSI}}$ exhibits a reliance on the absolute masses. Throughout this study, we have consistently assumed a value of $m_1$ equal to $10^{-5}$ eV. The corresponding values of $m_2$ and $m_3$ are then derived from the known quantities $\Delta m^2_{21}$ and $\Delta m^2_{31}$. The subsequent section features a presentation of probability plots along with a comprehensive description of the simulation methodology.

## 2.2 Details of statistical $\chi^2$ framework

Calculating $\chi^2$ helps us determine how well a theoretical idea matches actual experimental results. In simpler terms, $\chi^2$ tells us how much the real experimental data (the true data) differs from the data we'd expect based on the theory being tested (the test or fit data). In our study, we have developed the statistical framework using the long baseline simulator GLoBES. A detailed description of the GLoBES package and its modules has been added in the appendix B.

In our pursuit of constraining the absolute neutrino masses, we introduce a statistical measure, denoted by $\chi^2$, which serves as an indicator of sensitivity. This measure quantifies our ability to narrow down the possible neutrino mass values, taking into account the interplay between NSI effects and neutrino oscillations.

$$\chi^2_{pull} = \min_{\zeta_j} \left( \min_{\eta} \sum_i \sum_j \frac{\left[N^{i,j}_{true} - N^{i,j}_{test}\right]^2}{N^{i,j}_{true}} + \sum_{i=1}^{k} \frac{\zeta_i^2}{\sigma^2_{\zeta_i}} \right), \tag{2.19}$$

where, $N^{i,j}_{true}$ and $N^{i,j}_{test}$ represents the number of true and test events in the $\{i,j\}$-th bin respectively. Using the pull method described in [138, 139], we incorporate the systematic errors as additional parameters known as nuisance parameters $(\zeta_k)$ with the systematical errors $(\sigma^2_{\zeta_k})$. A detailed schematic for the event generation and $\chi^2$ calculation algorithm is shown in figure 2.1.

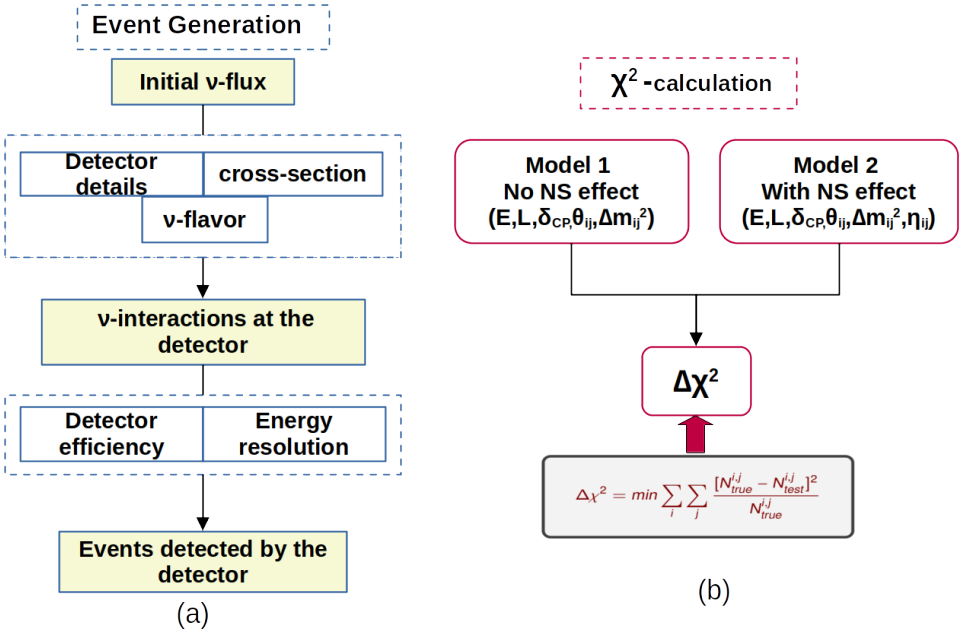


FIGURE 2.1: The methodology for studying detector sensitivity. (a) The methodology for event generation at the detector. (b) The framework for $\chi^2$ calculation.

## 2.3 Details of some upcoming neutrino experiments

We have presented a detailed examination of the technical specifications inherent to DUNE, T2HK, and T2HKK, offering an in-depth understanding of their individual characteristics. Furthermore, we have undertaken a comprehensive analysis, juxtaposing their respective baselines, L/E (distance-to-energy ratio), and fiducial volumes, all of which are conveniently tabulated for easy reference in table 2.2. This comparison provides a holistic view of the distinguishing attributes and operational contexts of these experimental setups.

### 2.3.1 Deep Underground Neutrino Experiment

The Deep Underground Neutrino Experiment (DUNE), an innovative endeavor [140–144], represents a forthcoming long-baseline neutrino experiment set to be situated in the United States. Positioned within the Long-Baseline Neutrino Facility (LBNF), the Near Detector for this experiment will be situated approximately 574 meters underground, at a distance of 60 meters from the neutrino beam source at Fermilab. Following their emission, neutrinos will traverse a distance of 1300 km to reach the Far Detector (FD), nestled within the Homestake Mine in South Dakota. The Far Detector is comprised of four modules, each featuring a liquid argon time projection chamber (LArTPC), collectively offering a substantial fiducial mass of 10kt. Employing the LArTPC technology, the detection process involves capturing the charge ionization stemming from neutrino interactions. This method ensures exceptional spatial resolution, energy precision, three-dimensional trajectory reconstruction, and the ability to discern particle tracks through analysis of energy loss patterns along these tracks. The neutrino beam necessary for DUNE's investigations will be generated at Fermilab, boasting a power of 1.2 MW-120 GeV, and will facilitate the delivery of an impressive $10^{21}$ proton-on-target (POT) annually. Anticipated to commence its operations in 2026, DUNE is poised to open new avenues for neutrino research, harnessing cutting-edge technologies and methodologies to expand our understanding of these elusive particles.

### 2.3.2 Hyper Kamiokande

Hyper Kamiokande (HK) [17] is a proposed next-generation underground Water Cherenkov (WC) detector which will be located near the town Kamioka in Japan's Gifu Prefecture. It is designed to address different unknowns of various fields of physics and astrophysics. It consists of a cylindrical detector having PMTs as active detectors on

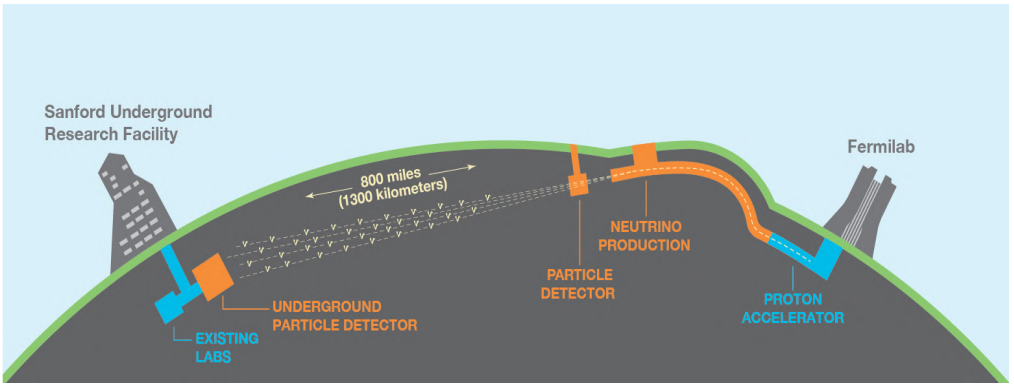


FIGURE 2.2: Schematic of the Deep Underground Neutrino Experiment (DUNE) [20].

its walls. The various parameters of the detector setup and its comparison with its predecessors (Kamiokande & Super-Kamiokande) are listed in Table 2.1. The HK detector is both a "microscope" used to observe elementary particles, and also a "telescope" for observing the Sun and supernovas, using neutrinos. The detector will also serve as a far detector for a long baseline neutrino experiment, referred as T2HK [83]. The neutrino beam for this experiment will be produced at the J-PARC (Japan Proton Accelerator Research Complex) facility and the baseline will be 295km. The Hyper-Kamiokande experiment employs a ring-imaging WC detector technique to detect rare interactions of neutrinos and the possible spontaneous decay of protons and bound neutrons. The construction of the HK detector is ongoing and is expected to start taking data from 2027.

### 2.3.3 Tokai to Hyper-Kamiokande

Tokai to Hyper-Kamiokande (T2HK), an ambitious endeavor [82], stands out as a significant long baseline experiment that holds great promise for advancing neutrino research. This experiment is meticulously designed to operate over a substantial baseline of 295 km. The operational framework entails the generation of a potent neutrino beam at the J-PARC facility, with detection taking place at the Hyper-Kamiokande (HK) detector. The neutrino beam from J-PARC endowed with a power of 1.3 MW, propels the generation of an impressive $27 \times 10^{21}$ proton-on-target (POT) annually. The HK detector, situated in Japan, represents a remarkable advancement from its predecessor, the Super-Kamiokande (SK) detector, boasting a fiducial mass roughly twenty times greater than that of Super-Kamiokande. Characterized by two cylindrical water Cherenkov modules, each boasting a fiducial mass of 187 kt, the HK detector is strategically placed at an angle of 2.5° off-axis from the J-PARC neutrino beam. In the context of our simulation studies, we have adopted a baseline of 295 km, and the fiducial volume is set at 374 kt,

| | Kamiokande | Super-Kamiokande | Hyper-Kamiokande |
|---|---|---|---|
| Depth | 1000m | 1000m | 650m |
| Height | 16m | 42m | 60m |
| Diameter | 15.6m | 39m | 74m |
| Volume | | | |
| *total* | 4.5kt | 50kt | 258kt |
| *inner* | 3kt | 32.5kt | 216kt |
| *fiducial* | 0.68kt | 22.5kt | 187kt |
| ID Photocoverage | 20 % | 40 % | 40 % |
| ID PMTs | 948 (50cm ) | 11129 (50cm ) | 40000 (50cm ) |
| OD PMTs | 123 (50cm ) | 1885 (20cm ) | 6700 (20cm ) |
| Single-photon detection efficiency | *unknown* | 12 % | 24 % |
| Single-photon timing resolution | 4ns | 23ns | 1ns |

TABLE 2.1: Comparison of Kamiokande, Super-Kamiokande and Hyper-Kamiokande specifications.

achieved through the deployment of two cylindrical detectors, each featuring a fiducial volume of 187 kt. The entire operational span spans a decade, distributed as 2.5 years in neutrino mode and 7.5 years in antineutrino mode, thereby maintaining a 1:3 ratio. This configuration ensures a balanced representation of both neutrino and antineutrino signal events within the experiment's data collection.

### 2.3.4 Tokai to Hyper-Kamiokande to Korea

Tokai to Hyper-Kamiokande to Korea (T2HKK) [83] emerges as another innovative configuration that branches from the T2HK initiative. Within this proposal, a distinctive plan materializes, involving the placement of the second cylindrical detector module from HK in Korea. Positioned at a considerable distance of 1100 km from the J-PARC proton synchrotron facility, this supplementary detector establishes the framework for the T2HKK experiment. Under the T2HKK configuration, two far detector set-ups are envisioned. The first, stationed at a distance of 295 km within the HK site, retains fidelity to the T2HK configuration. Meanwhile, the second detector, situated in Korea at the 1100 km mark, introduces an innovative dimension. Both of these detector modules encompass fiducial volumes of 187 kt, underpinned by the principles of the water

Cherenkov technique for neutrino detection. At an angular deviation of 2.5° from the neutrino beam axis, the detectors are meticulously positioned, thereby ensuring optimal data collection. It is noteworthy that the peak of the second oscillation maximum is projected to occur at an energy of 0.66 GeV.

In this study, it is imperative to note that we have adopted an approach where the background and systematic uncertainties inherent to the T2HKK setup mirror those attributed to the T2HK configuration. This strategy allows for a coherent and consistent analysis of both setups within our study framework.

| Experiment details | Channels | Normalization error | |
|---|---|---|---|
| | | Signal | Background |
| **DUNE** | | | |
| Baseline = 1300 km | $\nu_e(\bar{\nu}_e)$ appearance | 2 % (2%) | 5 % (5 %) |
| L/E = 1543 km/GeV | | | |
| Fiducial mass = 40 kt (LArTPC) | $\nu_\mu(\bar{\nu}_\mu)$ disappearance | 5 % (5 %) | 5 % (5 %) |
| Runtime = 3.5 yr $\nu$ + 3.5 yr $\bar{\nu}$ | | | |
| **T2HK** | | | |
| Baseline = 295 km | $\nu_e(\bar{\nu}_e)$ appearance | 3.2 % (3.9 %) | 10 % (10 %) |
| L/E = 527 km/GeV | | | |
| Fiducial mass = 187 × 2 kt (WC) | $\nu_\mu(\bar{\nu}_\mu)$ disappearance | 3.6 % (3.6 %) | 10 % (10 %) |
| Runtime = 2.5 yr $\nu$ + 7.5 yr $\bar{\nu}$ | | | |
| **T2HKK** | | | |
| Baseline = 295,1100km | $\nu_e(\bar{\nu}_e)$ appearance | 3.2 % (3.9 %) | 10 % (10 %) |
| L/E = 527,1964 km/GeV | | | |
| Fiducial mass = 187; 187 kt(WC) | $\nu_\mu(\bar{\nu}_\mu)$ disappearance | 3.6 % (3.6 %) | 10 % (10 %) |
| Runtime = 2.5 yr $\nu$ + 7.5 yr $\bar{\nu}$ | | | |

TABLE 2.2: Detector details and systematic uncertainties for different experiments.

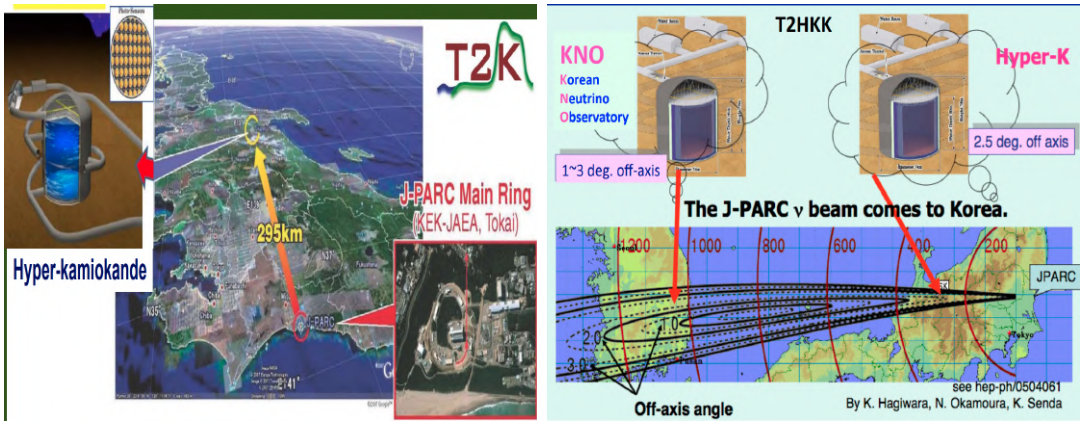


FIGURE 2.3: Schematics of T2HK (left) and T2HKK (right) experiments [21, 22].

## 2.4 Chapter Summary

In this chapter, we commence by providing an in-depth examination of the comprehensive framework encompassing various potential non-standard interactions (NSIs) of neutrinos. These NSIs serve as a compelling avenue for delving into novel physics within the leptonic sector. Subsequently, we delve into the formalism of scalar NSI, a realm that has garnered recent attention in the scientific literature. The impact of scalar NSIs manifests as a correction dependent on the nature of matter in relation to the neutrino mass term, rendering the exploration of its effects on diverse neutrino experiments particularly intriguing. Furthermore, we scrutinize the statistical framework adopted to assess the influence of NSIs on these neutrino experiments. To conclude, we provide an in-depth exploration of the specifics pertaining to various neutrino experiments incorporated into our simulation study.